The Journal of Chemical Physics

Stark-induced adiabatic Raman passage examined through the preparation of D_2 ($v = 2, j = 0$) and D_2 ($v = 2, j = 2, m = 0$)

Cite as: J. Chem. Phys. **150**, 234201 (2019); https://doi.org/10.1063/1.5109261
Submitted: 07 May 2019 . Accepted: 23 May 2019 . Published Online: 18 June 2019

William E. Perreault, Nandini Mukherjee, and Richard N. Zare

The Journal of Chemical Physics ARTICLE scitation.org/journal/jcp

Stark-induced adiabatic Raman passage examined through the preparation of D_2 ($v = 2, j = 0$) and D_2 ($v = 2, j = 2, m = 0$)

Cite as: J. Chem. Phys. 150, 234201 (2019); doi: 10.1063/1.5109261
Submitted: 7 May 2019 • Accepted: 23 May 2019 •
Published Online: 18 June 2019

William E. Perreault, Nandini Mukherjee,[a] and Richard N. Zare[a]

AFFILIATIONS

Department of Chemistry, Stanford University, Stanford, California 94305, USA

[a]Authors to whom correspondence should be addressed: nmukherj@stanford.edu and zare@stanford.edu

ABSTRACT

We study the conditions that must be met for successful preparation of a large ensemble in a specific target quantum state using Stark-induced adiabatic Raman passage (SARP). In particular, we show that the threshold condition depends on the relative magnitudes of the Raman polarizability (r_{0v}) and the difference of the optical polarizabilities ($\Delta\alpha_{00\to vj}$) of the initial ($v = 0, j = 0$) and the target (v, j) rovibrational levels. Here, v and j are the vibrational and rotational quantum numbers, respectively. To illustrate how the operation of SARP is controlled by these two parameters, we experimentally prepared D_2 ($v = 2, j = 0$) and D_2 ($v = 2, j = 2, m = 0$) in a beam of D_2 ($v = 0, j = 0$) molecules using a sequence of partially overlapping pump and Stokes laser pulses. By comparing theory and experiment, we were able to determine the Raman polarizability $r_{02} \approx 0.3 \times 10^{-41}$ Cm/(V/m) and the difference polarizabilities $\Delta\alpha_{00\to20} \approx 1.4 \times 10^{-41}$ Cm/(V/m) and $\Delta\alpha_{00\to22} \approx 3.4 \times 10^{-41}$ Cm/(V/m) for the two Raman transitions. Our experimental data and theoretical calculations show that because the ratio $r/\Delta\alpha$ is larger for the (0,0) → (2,0) transition than the (0,0) → (2,2) transition, much less optical power is required to transfer a large population to the ($v = 2$, $j = 0$) level. Nonetheless, our experiment demonstrates that substantial population transfer to both the D_2 ($v = 2, j = 0$) and D_2 ($v = 2, j = 2$, $m = 0$) is achieved using appropriate laser fluences. Our derived threshold condition demonstrates that with increasing vibrational quantum number, it becomes more difficult to achieve large amounts of population transfer.

INTRODUCTION

Scattering experiments probe molecular forces at the quantum level, but the amount of information that can be extracted from these experiments depends upon the precision with which the input quantum states are prepared.[1–4] To this end, quantum state preparation using optical fields has been widely deployed in the study of molecular collisions.[3–10] Stimulated Raman pumping is particularly suitable for the preparation of desired rovibrational quantum states of molecules having no permanent dipole moment in their electronic ground states.[11–13] However, in a collision-free environment like a supersonic beam, traditional optical excitation suffers from coherence-induced population oscillations between the initial and target states.[14,15] Adiabatic passage techniques were developed specifically to avoid these oscillations and thus consistently prepare a dense molecular sample in a desired target state.[15–22]

Adiabatic passage processes use a set of external parameters to carefully control the dressed or adiabatic eigenstates of the Hamiltonian under the influence of a slowly varying external field. Stark-induced adiabatic Raman passage (SARP) exploits the laser-induced Stark shift of a pair of strongly coupled molecular levels to manipulate the time evolution of the adiabatic eigenstates and achieve nearly complete population transfer to the target state.[15,21] We have previously demonstrated that the ($v = 0$) to ($v = 1$)[23–26] and ($v = 4$)[27] transitions in molecular hydrogen possess sufficiently strong Raman coupling for SARP to successfully transfer the entire ground state population to the target state using a pair of partially overlapping pump and Stokes pulses. Because SARP can prepare vibrationally excited eigenstates in many theoretically important molecules like

H_2, N_2, and CO using visible laser pulses, it is important to examine the threshold condition for successful population transfer to any desired vibrational level. With this goal in mind, we begin by briefly discussing the physics of a coherent optically coupled two-level system and then express the threshold condition for adiabatic passage in terms of the molecular parameters. We have previously described SARP using the Bloch-Feynman vector model,[15,21] but here we present an equivalent description using the time-varying adiabatic eigenstates.

We find that the threshold condition for SARP depends on two key parameters, the Raman polarizability (r_{0v}) and the difference of the optical polarizabilities ($\Delta\alpha_{00\to vj}$) of the initial ($v = 0$, $j = 0$) and the target (v, j) rovibrational levels. To illustrate how these two parameters determine the efficiency of SARP population transfer, we consider D_2 ($v = 0$) → ($v = 2$), one of the weaker Raman transitions in molecular deuterium. An earlier report on the preparation of D_2 ($v = 2$) using stimulated Raman pumping claimed that the coupling is too weak for SARP to work for this transition.[28] Contrary to this claim, our experimental results demonstrate preparation of the D_2 ($v = 2$) target level with nearly complete population transfer from the initial D_2 ($v = 0$, $j = 0$) ground state. By comparing with theoretical calculations, we have determined the Raman coupling coefficient and the difference polarizability for this transition. We then demonstrate how the relative magnitude of these two parameters influences the SARP population transfer by comparing the D_2 ($v = 0, j = 0$) → D_2 ($v = 2, j = 0$) and D_2 ($v = 0, j = 0$) → D_2 ($v = 2, j = 2, m = 0$) Raman excitations.

ADIABATIC POPULATION TRANSFER IN A TWO-LEVEL MOLECULAR SYSTEM

Let us consider an optically coupled two level system like that shown schematically in Fig. 1(a). The blue curve in Fig. 1(b) gives the characteristic saturation of the population transfer in the presence of the damping of the optically induced coherence, as would be the case in a high density gas bulb. The green curve shows resonant Rabi population oscillations, in which population transfer depends upon the energy of the optical pulse. Only the red curve, which shows the results of an adiabatic passage process, accomplishes consistent and complete population transfer. Below, we briefly discuss the equations of motion that govern population transfer in a coherent optically coupled two-level system. The discussion below follows that given by Shore[29] for adiabatic population transfer. After choosing the phase such that the energy zero is equal to the average energy of the bare states[29] and applying the rotating wave approximation, the system shown in Fig. 1(a) can be described by the Hamiltonian

$$H = \begin{bmatrix} -\Delta/2 & \Omega \\ \Omega & \Delta/2 \end{bmatrix}. \tag{1}$$

Here, $\Omega = p\mathscr{E}/\hbar$ is the Rabi frequency and Δ is the detuning, as shown in Fig. 1, that is, Δ goes to zero as the optical frequency passes through resonance. $\mathscr{E}$ and p are the slowly varying complex amplitudes of the optical field and the transition dipole moment connecting the initial and target states, respectively. The Hamiltonian in Eq. (1) describes the light-matter interaction in the absence of any dephasing of the optically induced coherence. After diagonalizing H, we get the adiabatic or optically dressed eigenstates, which can be expressed as

$$|+\rangle = \sin\theta|1\rangle + \cos\theta\,|2\rangle \tag{2}$$

and

$$|-\rangle = \cos\theta|1\rangle - \sin\theta|2\rangle, \tag{3}$$

where $|1\rangle$ and $|2\rangle$ refer to the unperturbed or bare initial and excited molecular energy states, as shown in Fig. 1(a). The angle θ is defined by $\cos\theta = \sqrt{\frac{\tilde{\Omega}+\Delta}{2\tilde{\Omega}}}$ and $\sin\theta = \sqrt{\frac{\tilde{\Omega}-\Delta}{2\tilde{\Omega}}}$, where $\tilde{\Omega} = \sqrt{\Delta^2 + 4\Omega^2}$.[29] The projection of the adiabatic states onto the bare states is defined by the angle θ. The two adiabatic eigenstates are indexed + and − in reference to the adiabatic energy eigenvalues $E_\pm = \pm\frac{\tilde{\Omega}}{2}$.[29]

Note that the Hilbert space of the adiabatic eigenstates is related to that of the bare states by a rotational transformation which depends on Ω and Δ and thus can be controlled by the parameters (intensity and frequency) of the optical field. Adiabatic passage transfers population via a single dressed state that slowly rotates from $|1\rangle$ to $|2\rangle$ in the two-dimensional Hilbert space spanned by the bare states. By examining the dynamics of the two-level system, we derive below three conditions that must be met for successful adiabatic population transfer.

Rabi oscillations

To begin, we examine the dynamics of Eqs. (1)–(3) under the sudden approximation where $\Omega = 0$ for $t < 0$ and $\Omega = c$ for $t \geq 0$,

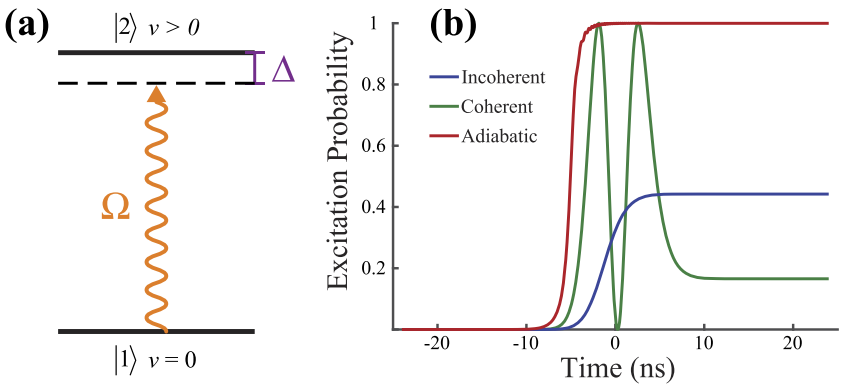

FIG. 1. (a) Schematic of the optical excitation of a two-level system. (b) Comparison of three different population transfer cases for the two level system shown in (a). The blue curve shows the characteristic saturation present in an incoherent system like a gas bulb. The green curve shows the Rabi oscillations in an uncontrolled coherent system, while the red curve shows the smooth population transfer of adiabatic passage that occurs with careful control of the optical pulses.

where c is a constant value not equal to zero. This is equivalent to abruptly turning on a continuous wave light source. Initially, at $t = 0$, the entire population resides in state $|1\rangle$. The initial state of the system can thus be expressed as a superposition of the adiabatic states $\psi(t = 0) = \sin\theta\,|+\rangle + \cos\theta\,|-\rangle$. At time $t > 0$, ψ will evolve as

$$\psi(t) = e^{i\tilde{\Omega}t/2}\sin\theta|+\rangle + e^{-i\tilde{\Omega}t/2}\cos\theta|-\rangle. \tag{4}$$

Taking the projection of $\psi(t)$ onto the bare state $|2\rangle$, we get an expression for the population of the target state $|2\rangle$ as a function of time

$$\begin{aligned}\rho_{22}(t) &= |C_2|^2 = |\langle 2|\,\psi\rangle|^2 = 4\cos^2\theta\sin^2\theta\sin^2\tilde{\Omega}t/2\\ &= \frac{4\Omega^2}{4\Omega^2+\Delta^2}\sin^2\tilde{\Omega}t/2,\end{aligned} \tag{5}$$

which can be easily recognized as the familiar Rabi oscillations shown by the green curve in Fig. 1(a). Equation (5) shows that population transfer depends upon the area $\int_0^t \tilde{\Omega}\ \mathrm{dt}$, which depends on the optical pulse energy. The Rabi population oscillations arise from the beating in time of the two adiabatic states, which results from the sudden change in $\Omega(t)$ that puts the system in a superposition of $|+\rangle$ and $|-\rangle$ at $t = 0$. Adiabatic passage achieves consistent population transfer by slowly varying $\Omega(t)$, thus ensuring that only a single adiabatic state is populated.

Adiabatic population transfer under slowly varying pulsed excitation $\Omega(t)$

We now consider pulsed excitation where $\Omega(t = 0) = 0$ and then $\Omega(t)$ slowly rises in time before eventually returning to zero. At $t = 0$ if Δ is large and positive and Ω is small, $\cos\theta \to 1$ and $\sin\theta \to 0$, and, thus $\psi(t = 0) \equiv |1\rangle$ coincides with the adiabatic state $|-\rangle$. At a later time, $t > 0$, $\psi(t)$ evolves as $\psi(t) = e^{-i\tilde{\Omega}t/2}|-\rangle$. As Ω grows in time, the population of the target state will rise as

$$\rho_{22}(t) = |C_2|^2 = |\langle 2|\,\psi\rangle|^2 = \sin^2\theta = \frac{\tilde{\Omega}-\Delta}{2\tilde{\Omega}}. \tag{6}$$

In Eq. (6) if the detuning does not change sign, that is to say, if Δ remains large and positive, then as Ω goes to zero, $\sin\theta \to 0$, and thus $C_2 \to 0$ at the end of the pulsed excitation with the system returning into the initial bare state $|1\rangle$. This is known as coherent population return,[15,19] where with the rise of the optical pulse, the population is transiently transferred to the target state but returns to the initial state as the pulse goes to zero. This occurs because the same adiabatic eigenstate coincides with the ground state before and after the optical excitation.

To achieve a unidirectional flow of population from $|1\rangle$ to $|2\rangle$, it is necessary to change the sign of Δ over the course of excitation, such that the populated adiabatic eigenstate coincides with $|1\rangle$ at the initial time and rotates smoothly in one direction in the Hilbert space to coincide with $|2\rangle$ at the end of the excitation. For example, if we start with a large positive Δ at $t = 0$, then the eigenstate $|-\rangle$ will initially align with the bare ground state $|1\rangle$ and rotate in the Hilbert space as Ω rises, maximally mixing the bare states $|1\rangle$ and $|2\rangle$ near the zero-crossing of Δ. As Δ becomes large and negative near the end of excitation [when $\Omega(t)$ returns to zero], $\cos\theta \to 0$ and $\sin\theta \to 1$. This 90° rotation of θ aligns the adiabatic state $|-\rangle$ with the bare state $|2\rangle$ at the end of the excitation process, thus transferring the entire population to the target state. Note that the adiabatic population transfer can be accomplished equally well if we start with a large negative Δ so the initial state $|1\rangle$ coincides with the adiabatic state $|+\rangle$.

The Landau-Zener condition for adiabatic population transfer

We noted above that any mixing of the adiabatic eigenstates will cause the population oscillations described above in Eqs. (4) and (5). Here, we show that mixing can be avoided as long as the speed of rotation $d\theta/dt$ of the adiabatic state is small compared to the rate of optical transition defined by the generalized Rabi frequency $\tilde{\Omega}$.[29] We first expand the state vector ψ in terms of the adiabatic eigenstates $\psi = A_+|+\rangle + A_-|-\rangle$. Using Eqs. (2) and (3), we can show that

$$\frac{d}{dt}\begin{bmatrix}A_+\\ A_-\end{bmatrix} = -i\begin{bmatrix}\tilde{\Omega}/2 & d\theta/dt\\ -d\theta/dt & -\tilde{\Omega}/2\end{bmatrix}\begin{bmatrix}A_+\\ A_-\end{bmatrix}. \tag{7}$$

Equation (7) shows that in order to keep the adiabatic states decoupled, $d\theta/dt \ll \tilde{\Omega}/2$. Using the definition of the projection angle θ, we derive the Landau-Zener condition[19,29]

$$\left|\Delta\frac{d\Omega}{dt} - \Omega\frac{d\Delta}{dt}\right| \ll \tilde{\Omega}^3/2. \tag{8}$$

The detuning can be swept in various ways using external static and optical fields. We show in the following that the criterion given in Eq. (8) is not absolutely strict and near complete population transfer is achieved in spite of slight mixing of the adiabatic eigenstates. Equation (8) sets up a threshold condition for the reduced Rabi frequency $\tilde{\Omega}$, which shows that with longer pulse duration, lower Rabi frequency and detuning will be required to satisfy the adiabaticity condition. Indeed, the minimum values of Δ and Ω are determined by the inverse pulse duration. For example, a 10 ns optical pulse will require both Δ and Ω to be on the order of 10^8 rad/s or greater for successful adiabatic passage. For SARP, Δ and Ω are determined by the intensity of the optical pulses, and so the adiabaticity condition requires a threshold intensity.

We summarize the conditions for successful adiabatic population transfer:

1. Only one of the adiabatic eigenstates must be populated at the initial time $t = 0$. This requires a slowly rising optical pulse such that at initial time $|\Delta| \gg \Omega$.
2. The populated adiabatic state must align with the target state at the end of the optical excitation. This requires the detuning Δ to change sign near the peak of the excitation defined by the Rabi frequency $\Omega(t)$. At the end of the optical pulse, we must have $|-\Delta| \gg \Omega$ in order to align the populated adiabatic state with the target state.
3. Consistent with the Landau-Zener condition, $\Delta(t)$ and $\Omega(t)$ must be varied sufficiently slowly in time so that the mixing of the adiabatic states is minimized.

As we show below with appropriate molecular parameters and laser fluences, SARP can satisfy the above three conditions using partially overlapping single mode optical pulses of nanosecond duration.

Stark-induced adiabatic Raman passage

As suggested by the name, SARP couples the ground and excited states using a two-photon resonant stimulated Raman linkage created by the laser pulses shown in Fig. 2(a). Because the SARP Raman transition involves far off-resonant intermediate states, it can be described by an equivalent two-level system to the one shown in Fig. 1(a).[30,31] The Rabi frequency for the two-photon Raman transition Ω_R is given by

$$\Omega_R = r_{0v}\frac{\mathscr{E}_P\mathscr{E}_S}{\hbar}, \tag{9}$$

where r_{02} is the Raman coupling of the $(v = 0) \rightarrow (v)$ Raman transition given by[13,21,31]

$$r_{0v} = \frac{1}{\hbar}\sum_k \mu_{0k}\mu_{kv}\left[\frac{1}{(\omega_{k0} - \omega_P)} + \frac{1}{(\omega_{k0} + \omega_S)}\right]. \tag{10}$$

Here, μ_{ik} are the transition dipole matrix elements, $\mathscr{E}_P$ and $\mathscr{E}_S$ are the slowly varying amplitudes of the optical fields defined by $E = \mathscr{E}e^{i\omega t} + c.c.$, and ω represents the circular frequency. By comparing Eq. (9) with the Rabi frequency defined above for Eq. (1), $r_{0v}\mathscr{E}_P$ can be recognized as the complex amplitude p of the transition dipole induced at the Stokes frequency. As such, r_{0v} can be identified as the Raman polarizability responsible for the spontaneous Raman scattering and can therefore be expressed in units of Cm/(V/m).

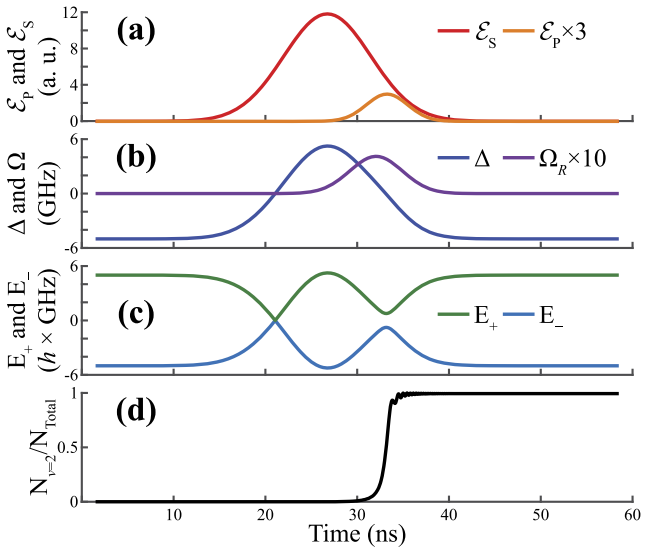

FIG. 2. Temporal dynamics of the SARP process. (a) Strong Stokes pulse (red) partially overlapping with a weaker pump pulse (orange). (b) The time dependent Stark detuning Δ (blue) induced by the stronger Stokes pulse, as well as the Rabi frequency Ω_R (purple) produced by the overlap of the pump and Stokes pulse. (c) The adiabatic energies E_+ and E_- as the Stokes and pump intensities rise and fall over the course of the excitation. (d) Complete population transfer to the ($v = 2$) state occurs in the presence of Ω_R near the second zero crossing of Δ. These plots were generated using the laser field parameters (fluence, pulse duration, detuning) present in our experiments and the molecular parameters (Raman coupling r_{02} and difference polarizability $\Delta\alpha_{00\rightarrow20}$) for the D_2 ($v = 0$) → ($v = 2$) Raman transition determined from the analysis of the experimental data (Figs. 3–7).

To sweep the detuning Δ through resonance, SARP takes advantage of the dynamic Stark shift of the molecular levels caused by intense pump and Stokes laser pulses shown in Fig. 2(a). The spectral width is thus determined by both the Raman coupling and the sweep rate of the two-photon detuning, which is given by $\Delta = \Delta_0 - \Delta_S$, where Δ_0 is the field-free or the static detuning and Δ_S is the Stark-induced detuning by the optical fields of the pump and Stokes laser pulses, given by[21]

$$\Delta_S = -\frac{\Delta\alpha(\omega_P)|\mathscr{E}_P|^2 + \Delta\alpha(\omega_S)|\mathscr{E}_S|^2}{\hbar}. \tag{11}$$

Here, $\Delta\alpha(\omega)$ gives the difference between the one-photon optical polarizabilities of the two resonant levels at frequency ω and is also expressed in units of Cm/(V/m).

Because the Stark shifted detuning will rise and fall with the intensity of the laser pulses, Δ will go through zero (resonance) twice, as shown by Fig. 2(a). As described above, each time Δ changes its sign, the adiabatic eigenstates make a 90° rotation in the Hilbert space. SARP avoids coherent population return during multiple zero-crossings of Δ by using a delayed sequence of pump and Stokes pulses with unequal intensities,[15,21] as shown by Fig. 2(a). Figure 2(b) shows the time-dependent detuning Δ as well as the Raman Rabi frequency Ω_R, which is present only during the second zero crossing of the detuning. Figure 2(c) shows the evolution of the adiabatic energies over the course of the optical pulses. Note that in the absence of Ω_R at the first zero-crossing of Δ, the adiabatic states cross; however, no population is transferred. During this crossing, because Δ changes sign while $\Omega_R = 0$, the adiabatic state that is aligned with the bare ground state rapidly switches, causing the population to hop from one adiabatic state to the other. Figure 2(d) shows that the entire population is transferred during the second zero crossing in the presence of the Rabi frequency Ω_R. During this crossing, the population remains trapped in the adiabatic state that is initially aligned with the ground state as it rotates through the Hilbert space of the bare states to coincide with the target state at the end of excitation. The second zero crossing is also known as the avoided crossing of the adiabatic eigenstates. Because Landau-Zener condition is nearly ideally satisfied, the mixing of the adiabatic states is minimal at the second crossing, making it possible to transfer population via a single adiabatic eigenstate $|+\rangle$ without causing large population oscillations. The small oscillations of the target state population seen in Fig. 2(d) are caused by slight unavoidable mixing of the adiabatic states.

Landau-Zener condition redefined for SARP

We now derive a relationship between the Raman coupling and the polarizability that satisfies the Landau-Zener condition for SARP population transfer. The condition defined in Eq. (8) to avoid nonadiabatic transitions is most stringent when the two adiabatic energies come closest, which occurs at $\Delta = 0$ as shown in Fig. 2(c). From Eq. (8), the near resonant ($\Delta \approx 0$) adiabaticity condition is thus

$$\frac{d\Delta}{dt} < 4\Omega^2. \tag{12}$$

Equation (12) defines the threshold Rabi frequency required to cross a resonance without exchanging population between the adiabatic eigenstates. We note that the condition given in Eq. (12) does not assure complete population transfer. To transfer population adiabatically while avoiding coherent population return (condition 2 above), SARP requires that the two optical pulses be of unequal intensities and be delayed with respect to one another. The dynamic Stark shift of the Raman transition in the SARP process is primarily caused by the more intense of the pump and Stokes pulses. Assuming a much stronger Stokes pulse, the Stark-induced detuning is closely approximated by

$$\Delta_S \approx -\frac{\Delta\alpha(\omega_S)|\mathscr{E}_S|^2}{\hbar}. \tag{13}$$

This approximation allows us to find a convenient rule of thumb expression for the adiabatic following condition. We note that for the numerical simulations presented in Figs. 3–9, we have calculated the Stark shifts due to both the stronger Stokes as well as the weaker pump pulse rather than using the above approximation.

To determine the sweep rate of the detuning, we assume a Gaussian intensity profile for the stronger Stokes pulse and find the maximum slope of the detuning Δ using the approximation given in Eq. (13). Thus, we estimate $\frac{d\Delta}{dt} = -\frac{2\Delta\alpha|\mathscr{E}_S|^2}{\hbar\tau_S}$, where τ_S gives the $1/e$ width of the intensity profile of the stronger pulse. To satisfy the adiabatic passage condition defined in Eq. (12), we require[13]

$$4\left|\frac{r_{0v}\mathscr{E}_P\mathscr{E}_S}{\hbar}\right|^2 > \frac{2\Delta\alpha|\mathscr{E}_S|^2}{\hbar\tau_S} \text{ or, } r_{0v} > \sqrt{\frac{\hbar\Delta\alpha}{2\tau_S|\mathscr{E}_P|^2}}. \tag{14}$$

Expressing r_{0v} and $\Delta\alpha$ in units of 10^{-41} Cm/(V/m) and expressing the electric field amplitude $\mathscr{E}_P$ in terms of the pump fluence ε_P in units of (J/cm^2), the Landau-Zener condition can be cast in the following form

$$r_{0v} > 2\sqrt{\frac{\Delta\alpha}{\varepsilon_P}}\sqrt{\frac{\tau_P}{\tau_S}}. \tag{15}$$

We would like to emphasize here that in Eqs. (14) and (15), we have assumed that the Stokes is the stronger of the two pulses. Thus, in Eq. (15), τ_P and ε_P refer to the $1/e$ width and the fluence, respectively, of the weaker laser pulse, while τ_S refers to the $1/e$ width of the stronger laser pulse. Equation (15) gives the constraint on the molecular parameters which must be met for the system to evolve adiabatically in the specific case of the SARP optical pulses given above in Fig. 2(a). We note that this condition alone is insufficient to assure population transfer using the SARP process. Conditions 1 and 2 above must also be met for successful adiabatic passage to occur. Additionally, significant population transfer can be achieved through Rabi cycling even when the condition given in Eq. (15) is not met.

SARP PREPARATION OF D_2 ($v = 2$, $j = 0$)

To prepare the D_2 ($v = 2$, $j = 0$, 2) rovibrational eigenstates, we combined a single mode 1064 nm Stokes pulse (~150 mJ, 11 ns FWHM) with a time-delayed, single-mode pump pulse at 655 nm (~30 mJ, 5 ns FWHM). The 1064 nm pulse was derived from an injection-seeded, Q-switched Nd^{+3}:YAG laser (PRO 290, Spectra Physics). The 655 nm pulse was derived from a three-stage pulsed dye amplifier (PulsAmp 5X-N, Sirah) seeded by a frequency stabilized single-mode, tunable dye laser (Matisse, Sirah). The pulse dye amplifier was pumped by the second harmonic of the same Nd^{+3}:YAG laser that generates Stokes pulse so that the arrival time of the pump and Stokes pulses is locked. Following an optical delay, the pump pulse was combined with the Stokes pulse on a dichroic beam splitter before being focused onto a supersonic beam of pure D_2 using a 60 cm focal length fused silica lens. We have used parallel polarization for the pump and Stokes optical fields. The SARP setup has been described in detail elsewhere.[23,24,27] The SARP prepared D_2 ($v = 2$) state was probed using (2 + 1) resonance-enhanced multiphoton ionization (REMPI) using tunable UV pulses near 213 nm. The UV pulses were derived from the third harmonic of a tunable pulsed dye laser (ND 6000, Continuum, Inc.) pumped by the second harmonic (532 nm) of a second Nd^{+3}:YAG laser (PL 9020, Continuum, Inc.). The delayed UV pulses were focused on the molecular beam using a 40 cm lens, slightly downstream (~0.4 mm) from the SARP excitation region.

Figure 3(a) shows the experimentally measured D_2 ($v = 2, j = 0$) REMPI signal as a function of the field-free detuning of the pump frequency from resonance for various pump (655 nm) fluences at a fixed Stokes (1064 nm) pulse fluence of 2500 J/cm^2 for a pump to Stokes delay of 6.5 ns. Note that the population of the target state is directly proportional to the REMPI signal from that state. Throughout the remainder of the paper, we will refer this spectral response as a function of the field-free detuning of the pump frequency as the SARP spectrum. Additionally, wherever we refer to the pump detuning, we mean the detuning of the pump from the field-free resonance frequency Δ_0. The peak height of the SARP spectrum as a function of the pump pulse fluence shows the saturation behavior that is characteristic of successful adiabatic passage.[27] Note that in the absence of dephasing of the induced Raman coherence, saturation of the measured REMPI signal of the target level occurs once the required threshold value of the Raman Rabi frequency or of the pulse fluence for adiabatic passage process is met. We will return to this condition later in the paper. Additionally, Fig. 3(a) shows that the SARP spectral width increases with the fluence of the pump pulse. This shows that at higher pump fluence, the adiabatic condition can be met over a broader range of the Raman detuning, making the population transfer more stable against the laser frequency fluctuations. Figure 3(b) compares the average peak of the various SARP spectra shown in Fig. 3(a) as a function of the pump fluence with the theoretically calculated population transfer using an estimated Stark detuning rate and Raman coupling coefficient. The strong correspondence between the simulations and the experimentally measured peak intensities shown in Fig. 3(b) suggests the fidelity of the estimated laser and molecular parameters used to calculate the $(v = 0) \rightarrow (v = 2)$ Raman transition.

Following the procedure developed in our earlier work,[15,21] the theoretical curves in Figs. 3–9 were calculated by numerically solving the time-dependent Schrödinger equation for the stimulated Raman two level system. To maximize the correspondence between the theoretical curves and experimental measurements shown in Fig. 3(b) as well as those shown in Figs. 4–6, we have varied the Raman coupling coefficient r_{02}. From the theoretical curves shown in Figs. 3–6, we could get a reasonably good estimate for the Raman coupling $r_{02} \approx 0.32 \times 10^{-41}$ Cm/(V/m) which includes the

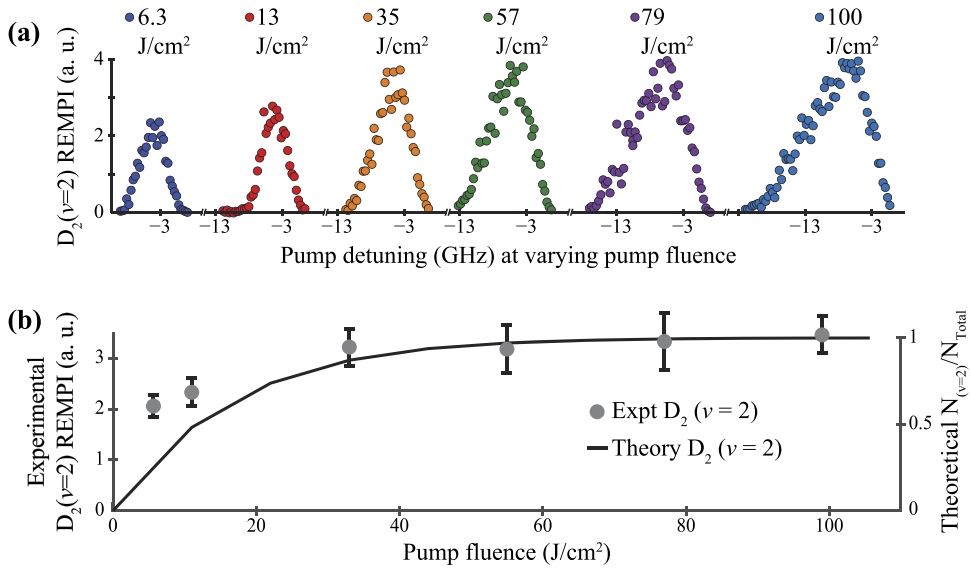

FIG. 3. Saturation of D_2 (v = 0, j = 0) → D_2 (v = 2, j = 0) Raman transition as a function of pump (655 nm) fluence (J/cm^2) at a pump to Stokes delay of 6.5 ns. (a) Spectral response of the REMPI signal from D_2 (v = 2, j = 0) as a function of the pump detuning (GHz) for various pump fluences at a fixed Stokes pulse fluence of 2500 J/cm^2. (b) Comparison of the theoretically calculated peak spectral response with that measured experimentally as a function of the pump fluence shown in (a).

Clebsch-Gordan coefficient for the (v = 0, j = 0) → (v = 2, j = 0) Raman transition.

To accurately describe the SARP process, our theoretical calculations took into account the dynamic Stark shifts induced by the pump and Stokes pulses.[15,21] As described in the section titled "Determination of $\Delta\alpha$ and evaluation of the Landau-Zener condition for SARP," we have extracted the difference polarizability $\Delta\alpha$ by measuring the Stark shift of the Raman transition. We have used Gaussian temporal profiles of the pump (5 ns FWHM) and Stokes (11 ns FWHM) intensities. The calculation of the instantaneous Raman Rabi frequency and net detuning required the pump and Stokes pulse fluences, which we have estimated using the measured spot sizes of the laser beam within the molecular beam. The spot sizes were experimentally determined from the spatial extent of the AC Stark shift of the D_2 (v = 0) REMPI transition induced separately by the pump and Stokes pulses.

Figures 4(a) and 4(b) show the SARP spectrum and the saturation of the peak intensity as a function of the pump fluence for the pump to Stokes delay of 3.5 ns. The theoretical curve shown in Fig. 4(b) is generated using the same Raman coupling and Stark detuning as the one in Fig. 3(b). A comparison with Fig. 3 shows that the 3 ns delay requires slightly more pump energy

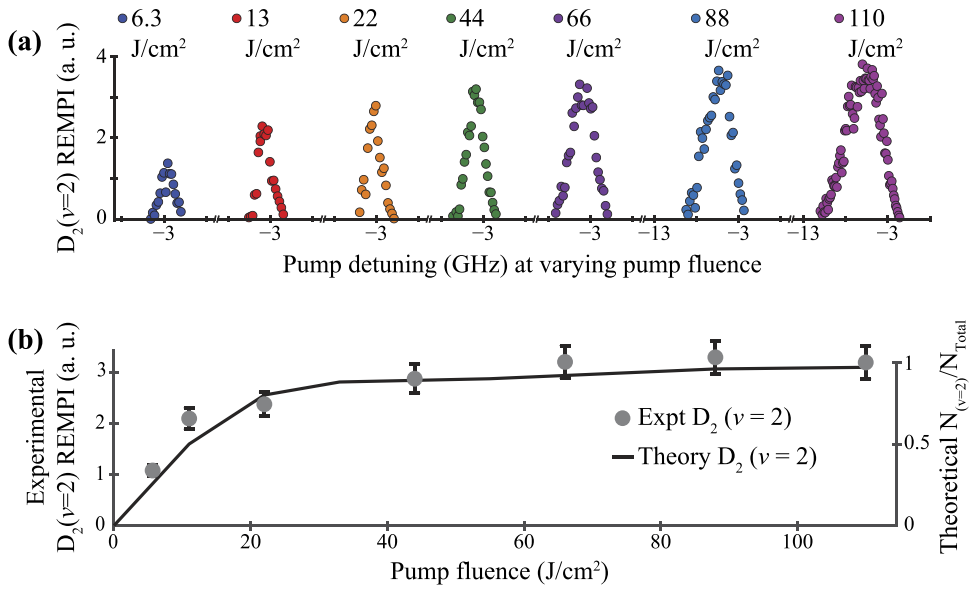

FIG. 4. Saturation of D_2 (v = 0, j = 0) → D_2 (v = 2, j = 0) Raman transition as a function of pump (655 nm) fluence (J/cm^2) at a pump to Stokes delay of 3.5 ns. (a) Spectral response of the REMPI signal from D_2 (v = 2, j = 0) as a function of the pump detuning (GHz) for various pump fluences at a fixed Stokes fluence of 2500 J/cm^2. (b) Comparison of the theoretically calculated peak spectral response with that measured experimentally as a function of the pump fluence shown in (a).

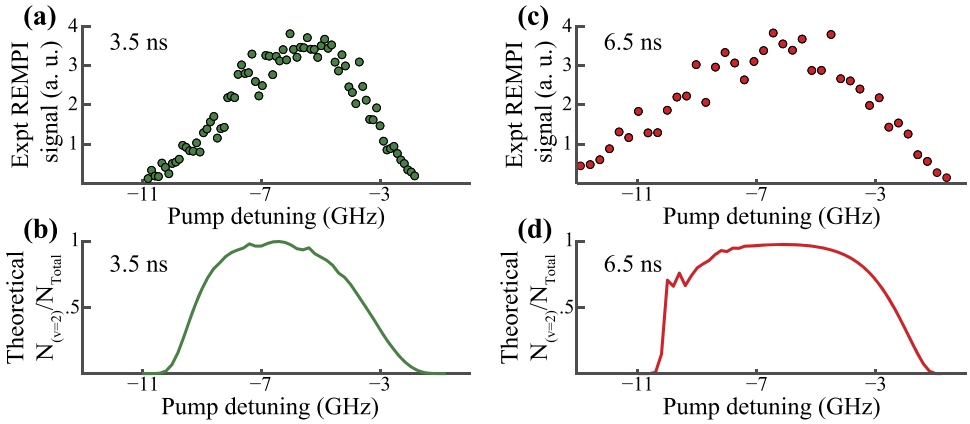

FIG. 5. Comparison of theoretically calculated and experimentally measured spectral response of the D_2 (v = 0, j = 0) → D_2 (v = 2, j = 0) Raman transition as a function of pump (655 nm) detuning (GHz) for two different pumps to Stokes delays. The top plots (a) and (c) present experimental SARP spectra for the delays of 3.5 ns (green dots) and 6.5 ns (red dots), respectively. The bottom plots (b) and (d) show the theoretically calculated spectra for the 3.5 ns (green curve) and 6.5 ns (red curve) delays, respectively. In all four plots, the Stokes fluence was 2500 J/cm^2. The pump fluence in (a) and (b) was 110 J/cm^2 for the delay of 3.5 ns, whereas in (c) and (d), for the delay of 6.5 ns, the pump fluence was 55 J/cm^2.

to saturate the REMPI signal. This is counterintuitive because at shorter delay, the Raman Rabi frequency will be stronger due to increased overlap of the pump and Stokes pulses. This behavior results because at shorter delay, the Raman transition samples the higher intensity portion of the stronger Stokes pulse, which increases the sweeping rate of the Stark detuning and thus requires higher pump fluence in order to satisfy the Landau-Zener condition.

Figure 5 compares the D_2 (v = 2, j = 0) SARP spectral response for 3.5 ns and 6.5 ns delays at respective pump fluences of 110 J/cm^2 and 55 J/cm^2. Even though twice as much pump fluence is used for the 3.5 ns delay, the SARP spectrum is clearly narrower. Figure 5 thus reinforces the fact that a longer pump to Stokes delay enhances the efficiency of SARP population transfer over a broader spectral range. Additionally, the reasonably strong correspondence between the theoretically calculated SARP spectra (bottom plots) and the experimentally determined SARP spectra (top plots) confirms the validity of the Raman coupling and Stark tuning parameters extracted from the experimental data.

Figure 6(a) presents experimental SARP spectra for various Stokes fluences for a fixed pump fluence of 79 J/cm^2 for the pump to Stokes delay of 6.5 ns. The spectral broadening and the saturation of the peak against Stokes pulse fluence again confirm the successful adiabatic passage. The excellent correspondence

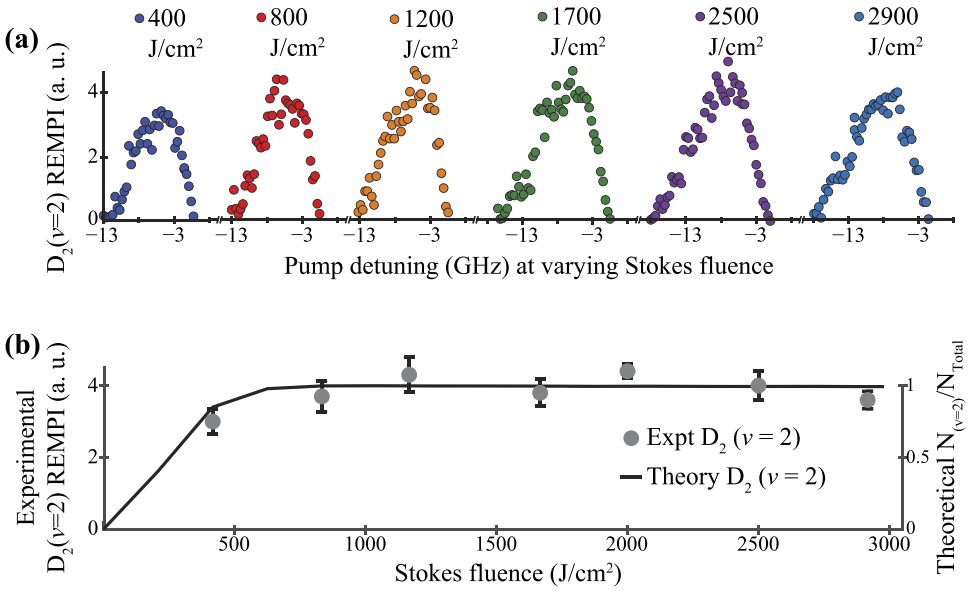

FIG. 6. Saturation of D_2 (v = 0, j = 0) → D_2 (v = 2, j = 0) Raman transition as a function of Stokes (1064 nm) fluence (J/cm^2) for a fixed pump fluence of 79 J/cm^2, at a pump to Stokes delay of 6.5 ns. (a) Experimentally measured spectral response of the REMPI signal from D_2 (v = 2, j = 0) as a function of the pump detuning (GHz) at various Stokes fluences. (b) Comparison of the theoretically calculated peak spectral response with that measured experimentally as a function of the Stokes fluence shown in (a).

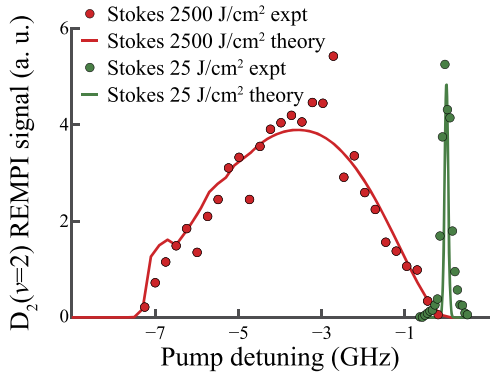

FIG. 7. Measurement of the dynamic Stark shift of the D_2 (v = 0, j = 0) → (v = 2, j = 0) Raman transition induced by the stronger (1064 nm) Stokes pulse. The red dots give the experimentally measured D_2 (v = 2, j = 0) spectrum for the strong Stokes field (2500 J/cm^2). The red solid curve is the theoretically calculated spectral response that closely describes the experiment. The green dots and green curve describe experimentally measured and theoretically calculated weak field spectra (Stokes fluence 25 J/cm^2), respectively. For both the strong and weak fields, the pump fluence was kept at 1 J/cm^2.

between the theoretically calculated population transfer and the experimentally determined peak intensities in Fig. 6(b) shows again the validity of the laser and molecular parameters used in the calculation.

DETERMINATION OF $\Delta\alpha$ AND EVALUATION OF THE LANDAU-ZENER CONDITION FOR SARP

The Stark tuning rate for the D_2 (v = 0, j = 0) → (v = 2, j = 0) Raman transition was precisely determined by measuring the Stark shift of the zero-field Raman resonance. Figure 7 shows two SARP spectra at the Stokes fluence of 25 and 2500 J/cm^2. The pump fluence was kept at 1 J/cm^2 for both spectra. For the weak pump and Stokes pulse energies, we obtain the narrow spectrum shown by the green dots and curve in Fig. 7 centered at the zero-field resonance of the (v = 0) → (v = 2) Raman transition in D_2, which corresponds to a pump frequency of 457 563 GHz. The zero-field Raman resonance was found to be 175.922 THz or 5868.12 cm^{-1}, which is within 100 MHz of a prior theoretical prediction of the energy difference for this transition.[32] The spectrum at higher Stokes fluence of 2500 J/cm^2 is broadened by the Stark shift of the Raman transition induced by the intense Stokes pulse, thus allowing us to calculate the difference polarizability $\Delta\alpha$. By matching theoretically calculated spectra to our experimental data, we estimate a Stark shift rate of ~41 MHz/(GW/cm^2) as a function of the Stokes laser intensity. This Stark shift rate corresponds to a difference polarizability $\Delta\alpha_{00\to20} \approx 1.4 \times 10^{-41}$ Cm/(V/m) between the (v = 0, j = 0) and (v = 2, j = 0) levels. The blue curve in Fig. 2(b) shows the Stark-induced detuning as a function of the pulse time for the SARP process using this Stark shift rate.

For the difference polarizability $\Delta\alpha_{00\to20} \approx 1.4 \times 10^{-41}$ Cm/(V/m) extracted from the Stark shift measurement and with $\tau_P/\tau_S \approx 1/2$ and ε_P = 100 J/cm^2, a minimum Raman coupling of $r_{02} > 0.17 \times 10^{-41}$ Cm/(V/m) would be necessary to satisfy the condition given in Eq. (15). Note that our extracted Raman coupling for the transition is nearly double the required value. For $r_{02} \approx 0.32 \times 10^{-41}$ Cm/(V/m), we find that the minimal energy of the pump pulse required for complete population transfer is ~30 J/cm^2. This explains the saturation behavior against pump pulse energies seen in Figs. 3 and 4. In general, the adiabatic passage process is very forgiving. Consequently, a reasonably large population may be transferred to the target state even if the Landau Zener condition is barely satisfied, as we will see below.

SARP PREPARATION OF D_2 (v = 2, j = 2, m = 0)

To further demonstrate the significance of the adiabaticity condition expressed in Eq. (15), we have studied the D_2 (v = 0, j = 0)

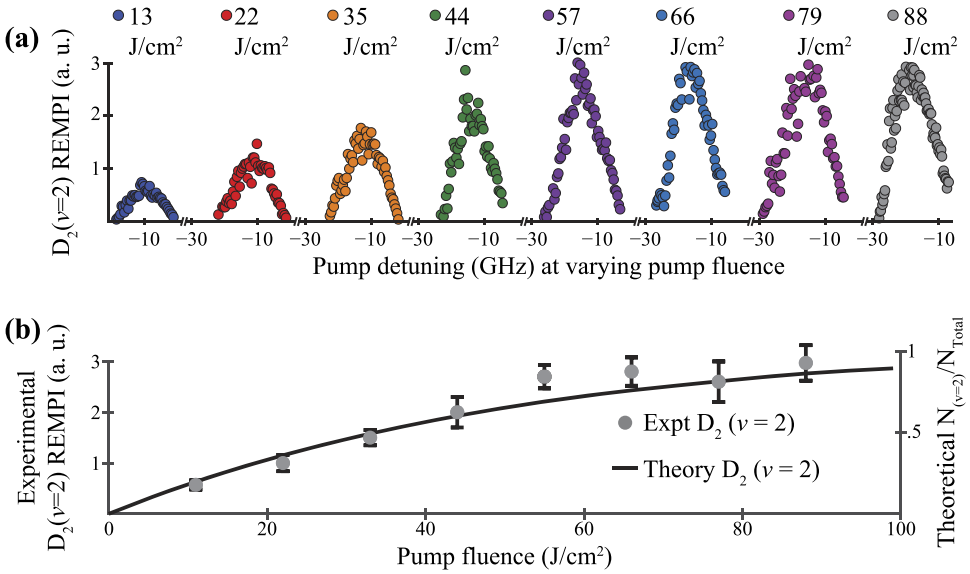

FIG. 8. Saturation of D_2 (v = 0, j = 0) → D_2 (v = 2, j = 2, m = 0) Raman transition as a function of pump (655 nm) fluence (J/cm^2) at a pump to Stokes delay of 6.5 ns. (a) Spectral response of the REMPI signal from D_2 (v = 2, j = 2) as a function of the pump detuning (GHz) for various pump fluences at a fixed Stokes fluence of 2500 J/cm^2. (b) Comparison of the theoretically calculated peak spectral response with that measured experimentally as a function of the pump fluence shown in (a).

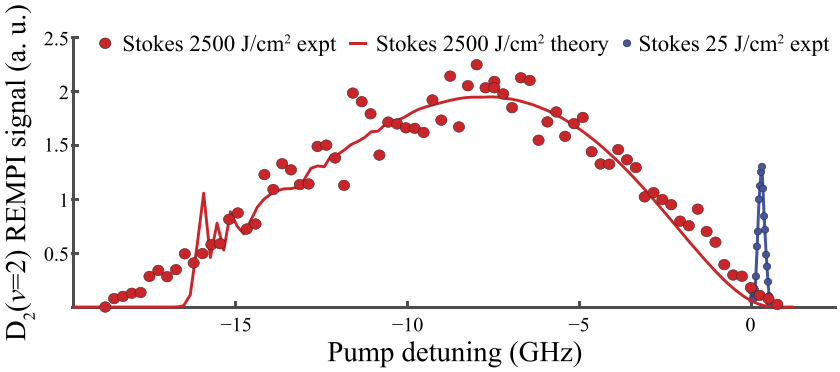

FIG. 9. Measurement of the dynamic Stark shift of the D_2 ($v = 0$, $j = 0$) → ($v = 2$, $j = 2$, $m = 0$) Raman transition induced by the stronger (1064 nm) Stokes pulse. The red dots give the experimentally measured D_2 ($v = 2$, $j = 2$) spectrum for the strong Stokes field (2500 J/cm^2). The red solid curve is the theoretically calculated spectral response that closely describes the experiment. The blue dots describe experimentally measured weak field spectra (Stokes fluence of 25 J/cm^2). The blue solid curve serves only as a guide connecting the experimentally measured points. For both the strong and weak fields, the pump pulse fluence was kept at 1 J/cm^2.

→ ($v = 2$, $j = 2$, $m = 0$) excitation using SARP. We note that because we have used parallel polarizations for the pump and Stokes lasers, the D_2 ($v = 2$, $j = 2$, $m = 0$) bond axis is aligned parallel to the laser polarization axis. Figure 8(a) shows the D_2 ($v = 0$, $j = 0$) → ($v = 2$, $j = 2$, $m = 0$) SARP spectra for various pump fluences at a fixed Stokes pulse fluence of 2500 J/cm^2. As opposed to the D_2 ($v = 0, j = 0$) → ($v = 2, j = 0$) SARP spectra shown in Figs. 3(a) and 4(a), Fig. 8(a) shows a much weaker saturation of the peak spectral response against the pump pulse energy.

To explain the weaker saturation in terms of the Landau-Zener condition, we determined the difference polarizability for the D_2 ($v = 0, j = 0$) → ($v = 2, j = 2, m = 0$) Raman transition using the spectra shown in Fig. 9. By comparing theory with the experimental data, we found $\Delta\alpha \approx 3.4 \times 10^{-41}$ Cm/(V/m) for this transition, which is nearly 2.5 times larger than the value found for the ($v = 0, j = 0$) → ($v = 2, j = 0$) Raman transition. To satisfy condition given in Eq. (15) using the same pump and Stokes fluences, this $\Delta\alpha$ will require a minimum Raman coupling $r_{02} > 0.26 \times 10^{-41}$ Cm/(V/m). Compared to the D_2 ($v = 0, j = 0$) → ($v = 2, j = 0$) transition, the Raman coupling r for the ($v = 2, j = 2, m = 0$) transition is reduced by a factor of $\sqrt{4/5}$. With $r_{02} \approx 0.29 \times 10^{-41}$ Cm/(V/m), the Landau-Zener condition is barely satisfied, making it harder to saturate as demonstrated by both the experimental and theoretical curves in Fig. 8(b).

CONCLUSION

We have examined the conditions required to achieve nearly complete population transfer to a desired rovibrational energy state using SARP with a pair of partially overlapping optical pulses. We have shown that in addition to the laser field parameters such as the frequency, delay, and ratio of the fluences that can be optimized by the experimentalist, the SARP efficiency sensitively depends upon two key molecular parameters, the difference polarizability $\Delta\alpha$ and the two-photon Raman coupling r. We redefined the Landau-Zener condition in terms of the relative magnitude of these two parameters and have shown how they control the operation of SARP. To critically evaluate the significance of these parameters, we have experimentally studied the preparation of D_2 ($v = 2$, $j = 0$) and D_2 ($v = 2$, $j = 2$) using nanosecond laser pulses with fluences in the range of 30–3000 J/cm^2. By comparing detailed theoretical calculations with experimental data, we were able to extract the Raman coupling and the difference polarizabilities for the D_2 ($v = 0$, $j = 0$) → D_2 ($v = 2$, $j = 0, 2$) transitions. We find that while the value of $r_{02} \approx 0.3 \times 10^{-41}$ Cm/(v/m) is nearly the same for the two transitions, $\Delta\alpha$ differs by more than a factor of two, with $\Delta\alpha_{00\to20} \approx 1.4 \times 10^{-41}$ Cm/(V/m) and $\Delta\alpha_{00\to22} \approx 3.4 \times 10^{-41}$ Cm/(V/m).

In spite of the large values of $\Delta\alpha$ for the two transitions studied here, our data clearly demonstrate that nearly complete population transfer from D_2 ($v = 0$, $j = 0$) to D_2 ($v = 2$, $j = 0$) and D_2 ($v = 2$, $j = 2$) was achieved. As pointed out in the Introduction, our experimental observation contradicts the results of the earlier study that concluded that SARP does not work for the D_2 ($v = 0, j = 0$) to D_2 ($v = 2, j = 0$) transition based on the fact that the maximum population transfer drops with increasing delay.[28] As we have described in great detail, successful population transfer using SARP depends sensitively on the amplitudes of the pump and Stokes optical fields. It is impossible for us to directly compare our results with those obtained in the earlier study because no specific information on the laser fluences in that experiment was given. Nonetheless, we can say definitively that careful control over the pump and Stokes fluences is required to both maintain adiabaticity and avoid population return near zero delay. In the absence of such fine control, a finite population can always be transferred at zero delay using Rabi cycling with mixed adiabatic states, which can be achieved simply by using a low fluence for the weaker laser pulse.

Our experimental data and theoretical calculations both clearly demonstrate that because of the higher value of $\Delta\alpha$ for the rotationally aligned D_2 ($v = 2$, $j = 2$, $m = 0$) state, the ($v = 0$, $j = 0$) → ($v = 2$, $j = 2$, $m = 0$) transition requires higher pump intensity to saturate the population transfer. We have shown that reduced population transfer caused by the mixing of the adiabatic eigenstates is unavoidable when the Stark tuning rate, which is determined by $\Delta\alpha$, exceeds a certain maximum value set by the Raman coupling and other experimental parameters defined in Eq. (15). Because,

in general, $\Delta\alpha$ will increase as the vibrational quantum number of the target state increases while the Raman coupling r will degrade, the relationship of $\Delta\alpha$ and r becomes even more important for the preparation of higher vibrational levels. Although the relationship given by Eq. (15) is specific to the SARP process, the efficiency of population transfer for any Stark-induced adiabatic passage process is determined by the relative magnitude of the multiphoton coupling coefficient and the difference polarizability between the initial and target levels.

ACKNOWLEDGMENTS

This work has been supported by the U.S. Army Research Office under ARO Grant Nos. W911NF-16-1-1061, W911NF-19-1-0163, and W911NF-19-1-0283. The authors thank Haowen Zhou for his help in the lab.

REFERENCES

[1] R. N. Zare, "Laser control of chemical reactions," Science **279**, 1875–1879 (1998).
[2] R. V. Krems, "Cold controlled chemistry," Phys. Chem. Chem. Phys. **10**, 4079–4092 (2008).
[3] W. E. Perreault, N. Mukherjee, and R. N. Zare, "Quantum control of molecular collisions at 1 Kelvin," Science **358**, 356–359 (2017).
[4] W. E. Perreault, N. Mukherjee, and R. N. Zare, "Quantum controlled rotationally inelastic scattering of HD with H_2 and D_2 near 1 Kelvin reveals collisional partner reorientation," Nat. Chem. **10**, 561–567 (2018).
[5] E. A. Rohlfing, D. W. Chandler, and D. H. Parker, "Direct measurement of rotational energy transfer rate constants for HCl (v = 1)," J. Chem. Phys. **87**, 5229–5237 (1987).
[6] P. Dittmann *et al.*, "The effect of vibrational excitation ($3 \leq v' \leq 19$) on the reaction Na_2 (v')+Cl→NaCl+Na*," J. Chem. Phys. **97**, 9472 (1992).
[7] K. Liu, "Perspective: Vibrational-induced steric effects in bimolecular reactions," J. Chem. Phys. **142**, 080901 (2015).
[8] M. H. G. de Miranda *et al.*, "Controlling the quantum stereodynamics of ultracold bimolecular reactions," Nat. Phys. **7**, 502–507 (2011).
[9] S. Ospelkaus *et al.*, "Quantum-state controlled chemical reactions of ultracold potassium-rubidium molecules," Science **327**, 853–857 (2010).
[10] B. L. Yoder, R. Bisson, and R. D. Beck, "Steric effects in the chemisorption of vibrationally excited methane on nickel," Science **329**, 553–556 (2010).
[11] W. Meier, G. Ahlers, and H. Zacharias, "State selective population of H_2 ($v'' = 1$, $J'' = 1$) and D_2 ($v'' = 1$, $J'' = 2$) and rotational relaxation in collisions with H_2, D_2, and He," J. Chem. Phys. **85**, 2599 (1986).
[12] R. Dopheide and H. Zacharias, "Rotational alignment by stimulated Raman pumping: C_2H_2 ($v'_2 = 1$, J')," J. Chem. Phys. **99**, 4864–4866 (1993).
[13] N. Mukherjee, W. E. Perreault, and R. N. Zare, "Stark-induced adiabatic passage processes to selectively prepare vibrationally excited single and superposition of quantum states," in *Frontiers and Advances in Molecular Spectroscopy* (Elsevier, Inc., 2018), pp. 1–46.
[14] B. W. Shore, "Elementary atoms," in *The Theory of Coherent Atomic Excitation* (John Wiley & Sons, 1990), pp. 93–186.
[15] N. Mukherjee and R. N. Zare, "Can stimulated Raman pumping cause large population transfers in isolated molecules," J. Chem. Phys. **135**, 184202 (2011).
[16] E. B. Treacy, "Adiabatic inversion with light pulses," Phys. Lett. A **27**, 421–422 (1968).
[17] M. M. T. Loy, "Observation of population inversion by optical adiabatic rapid passage," Phys. Rev. Lett. **32**, 814–817 (1974).
[18] D. Grischkowsky and M. M. T. Loy, "Self-induced adiabatic rapid passage," Phys. Rev. A **12**, 1117–1120 (1975).
[19] N. V. Vitanov, M. Fleischhauer, B. W. Shore, and K. Bergmann, "Coherent manipulation of atoms and molecules by sequential laser pulses," Adv. At., Mol., Opt. Phys. **46**, 55–190 (2001).
[20] N. V. Vitanov, T. Halfmann, B. W. Shore, and K. Bergmann, "Laser-induced population transfer by adiabatic passage techniques," Annu. Rev. Phys. Chem. **52**, 763–809 (2001).
[21] N. Mukherjee and R. N. Zare, "Stark-induced adiabatic Raman passage for preparing polarized molecules," J. Chem. Phys. **135**, 024201 (2011).
[22] H. Chadwick, P. M. Hundt, M. E. van Reijzen, B. L. Yoder, and R. D. Beck, "Quantum state specific reactant preparation in a molecular beam by rapid adiabatic passage," J. Chem. Phys. **140**, 034321 (2014).
[23] N. Mukherjee, W. Dong, J. A. Harrison, and R. N. Zare, "Communication: Transfer of more than half the population to a selected rovibrational state of H_2 by Stark-induced adiabatic Raman passage," J. Chem. Phys. **138**, 051101 (2013).
[24] W. Dong, N. Mukherjee, and R. N. Zare, "Optical preparation of H_2 rovibrational levels with almost complete population transfer," J. Chem. Phys. **139**, 074204 (2013).
[25] T. Wang, T. Yang, C. Xiao, D. Dai, and X. Yang, "Highly efficient pumping of vibrationally excited HD molecules via Stark-induced adiabatic Raman passage," J. Phys. Chem. Lett. **4**, 368–371 (2013).
[26] T. Wang, T. G. Yang, C. L. Xiao, D. X. Dai, and X. M. Yang, "Efficient coherent population transfer of D_2 molecules by Stark-induced adiabatic Raman passage," Chin. J. Chem. Phys. **26**, 8–12 (2013).
[27] W. E. Perreault, N. Mukherjee, and R. N. Zare, "Preparation of a selected high vibrational energy level of isolated molecules," J. Chem. Phys. **145**, 154203 (2016).
[28] T. Yang *et al.*, "Efficient preparation of D_2 molecules in $v = 2$ by stimulated Raman pumping," Chin. J. Chem. Phys. **30**, 614–618 (2017).
[29] B. W. Shore, "The Schrodinger atom," in *The Theory of Coherent Atomic Excitation* (John Wiley & Sons, 1990), pp. 187–262.
[30] N. Mukherjee, "Graphical technique for the calculation of nonlinear optical polarization," J. Opt. Soc. Am. B **23**, 1635 (2006).
[31] S. Chelkowski and A. D. Bandrauk, "Raman chirped adiabatic passage: A new method for selective excitation of high vibrational states," J. Raman Spectrosc. **28**, 459–466 (1997).
[32] J. Komasa *et al.*, "Quantum electrodynamics effects in rovibrational spectra of molecular hydrogen," J. Chem. Theory Comput. **7**, 3105–3115 (2011).